Journal of Advanced Scientific Research
Available online through https://sciensage.info
ISSN
0976-9595
Research Article

NATURAL DYE SENSITIZED SOLAR CELLS USING HENNA LEAVES WITH ZnO NANOPARTICLE AT VARIOUS pH VALUES

Selva Esakki*[1], Kamatchi Devi[2], Sheeba[2], Meenakshi Sundar[2]
[1]*Research Scholar (Reg.No 12441), PG and Research Department of Physics, Sri Paramakalyani College, Alwarkurichi, Affiliated to Manonmaniam Sundaranar University, Abishekapatti, Tirunelveli, Tamilnadu, India*
[2]*PG and Research Department of Physics, Sri Paramakalyani College, Alwarkurichi, India*
**Corresponding author: selvaesakki7270@gmail.com*
Received: 22-02-2022; Accepted: 20-05-2022; Published: 30-06-2022
 https://doi.org/10.55218/JASR.202213507

ABSTRACT
In this research, ZnO nanoparticles were synthesized at different pH values (3, 6 and 9) by using solvothermal method. To our knowledge, dye sensitized solar cells were fabricated using natural dyes extracted from henna (*Lawsonia Inermis*) based on ZnO nanoparticle as photoanode at various pH values. Synthesized ZnO samples were characterized using X-Ray Diffraction (XRD), Field Emission Scanning Electron Microscope (FESEM) with Energy Dispersive X-ray Spectroscopy (EDX), UV-Visible Spectroscopy and Fourier Transmission Infra-Red Spectroscopy (FTIR) and absorbance and transmittance properties of the prepared samples were investigated. The ZnO at pH 9 was obtained highest efficiency extracted from henna (*Lawsonia Inermis*) of 0.39% better than the other solar cells of pH variations.

Keywords: Energy conversion, Photovoltaics, Solar cells.

1. INTRODUCTION
In later a long time, Dye-Sensitized Solar Cells (DSSCs) based on ZnO nanoparticles have attracted considerable attention because of their low cost and facile fabrication procedures [1]. At present, they have become a potentially low-cost, efficient alternative to the conventional silicon p-n junction solar cells on the market. Generally, DSSC contains five components; 1). Transparent conducting oxide (TCO), 2). Semi-conductor metal oxide (ZnO) 3). Sensitizer (Dye molecule), 4). Electrolyte (redox couple) and 5).Counter electrode. These are the components that convert light energy into electrical energy. ZnO is one of the most important functional semiconductors and is a very attractive material having many applications including dye-sensitized solar cells, UV laser, biosensors, bio-imaging, drug delivery, piezoelectric transducers, high sensitivity chemical gas sensor, volatile organic compound sensor [2]. ZnO is an environment friendly material. The advantages of using ZnO over TiO_2 are its direct bandgap (3.37 eV) higher exciton binding energy (60meV) compared to TiO_2 (4meV) making it better at absorbing visible light. Besides, it is also more stable towards photo-corrosion [3]. Then ZnO nanoparticles have been synthesized by different techniques like sol-gel, chemical bath deposition, solvothermal, powder technique, electrodeposition, green synthesis and precipitation method [4]. Solvothermal process is a irradiation microwave technique. It is easier and cheaper compared to other methods. Yet resulting in almost comparable results it has been used for the synthesis of ZnO nanomaterials. Therefore, in this research, ZnO was synthesized by solvothermal process using zinc acetate, urea and ethylene glycol as solvent. It has the potential advantages of short reaction time, production of small particles, with narrow size distribution and high purity [5, 6]. Next, the performance of the cell mainly depends on a dye used as a sensitizer. The absorption of the dye on the surface of ZnO is significant parameter found the efficiency of the solar cell [7]. Generally, DSSC are prepared using synthetic dyes. However, there are disadvantages with these dyes because of high cost, their toxic nature, small colors and stability issues in the longer run. The advantages of natural dyes are several colors, low cost, high stability. Many researchers have been utilizing kinds of natural dyes. But the biggest

challenge is that DSSCs fabricated using natural dyes have shown very low efficiency compared to synthetic dyes [8]. In like manner, research has been centered around elective, effectively accessible photo sensitizers extracted from natural sources due to its low cost, simple extraction, higher effectiveness, enormous absorption coefficients and climate changes [7]. It has been reported for that, natural dyes can be handily extracted from various plants, for example, yellow marigold, pomegranate, Alpinia, grape pomace, henna leaves, mango leaves, red calico leaves, Rosella and blue pea blossoms.

To extract these natural dyes specific techniques such as magnetic stirring, ultrasound-assisted extraction, subcritical water extraction, soxhlet process and supercritical fluid extraction are suggested to increase the dye yield [9]. These natural dyes contain hydroxyl groups, are mostly water-soluble and usually contain various pigments, including chlorophyll, carotene, anthocyanin, betacyanin and phycocyanins in the flowers, petal or plant leaves [10]. The use of extraction enhancement and different pigment functions in different characteristic pigment activities are constantly being researched. However, it is imperative to improve extraction techniques to identify the right strategy for various artificial dye applications. These extractions of natural dyes affect the performance of solar cell due to several colors, pigment groups, etc. There are many studies in practice that use natural dyes as a sensitizing tool. But the downside is that they have an efficiency of less than 1%. This problem can be circumvented by identifying natural dyes which increase the performance efficiency [11]. In this context, chlorophyll pigment is found in the leaves of henna and pongame was examined on the leaves of '*Lasonia inermis*' (henna plant). Chlorophyll pigment is also obtained from all green leaves. The leaves of the Henna plant contain a characteristic and exceptionally compelling color: This orange / red dye has been practiced as a beauty product for mankind for over 5000 years with its crushed leaves.

In this work, ZnO nanoparticle have been prepared by using solvothermal method at various pH (3, 6 & 9) values which were employed as photoanode for DSSCs. The natural dyes were extracted from Henna leaves with ethanol as solvent. The J-V characterization was carried out to analyze the solar conversion efficiency of the fabricated DSSCs. To the best performance of DSSC fabricated from different pH -ZnO photoanodes was investigated.

2. MATERIAL AND METHODS

2.1. Material

Henna (*Lawsonia inermis*) used in this study were collected from Alwarkurichi City. Iodolyte was purchased from Solaronix Egypt. HCl and acetic acid were purchased from Madurai. Isopropanol was purchased from Madras Scientific Tirunelveli. FTO conductive glass (sheet resistance: 7Ω/sq), purchased from Technistro, Nagpur, Maharashtra. Zinc acetate dehydrate, ethylene glycol and urea were purchased from Madras scientific.

2.2. Preparation of Zno with different pH values nanoparticles by Solvothermal method

Analytical grade precursor materials such as Zinc acetate dihydrate, Urea (H_2NCONH_2) were used to synthesize ZnO nanoparticles by solvothermal method. Ethylene glycol ($CH_2OH.CH_2OH$) was utilized as a dissolvable. Three samples were synthesized for the present study by varying the pH values of the solution (3, 6, and 9). In this process, Zinc acetate dihydrate and urea in the 1:3 ratios were mixed well with ethylene glycol and the mixture was stirred well for 1hr using a magnetic stirrer. The stirrer solution in a bowl was placed in a domestic microwave oven at a temperature of 80°C. The ZnO solution was microwave treated until the dissolvable dissipated completely. Further, the substance deposited in the bowl was taken out and washed at least four times with double distilled water and acetone to remove unwanted water-soluble compounds and organic compounds present in the samples. The synthesized nanoparticles were filtered, dried in sunlight for one week and annealed in a muffle furnace at 500°C for 2hrs to improve the crystallinity of samples [12-16].

2.3. Preparation of Dye Sensitized Solar Cell (DSSC)

The conductive glass substrates were Fluorine doped Tin Oxide (FTO) with a sheet resistance of 15 Ohms/sq dimensions 25mm×25mm×2.2mm (L×W×T). The samples were cleaned in a detergent solution using an ultrasonic bath for 10min, rinsed with distilled water and ethanol and then dried. The ZnO paste was prepared by adding 3.5gm of ZnO nanopowder, 1ml acetic acid, 4ml of ethanol, 5ml of distilled water and 2 drops of Triton X-100. The mixture was then ground for half an hour until a homogeneous paste appeared. ZnO paste was coated on the FTO conductive glass plate by using doctor blade technique (rolling of glass rod on the FTO glass substrate) [17-20]. The area of the coated glass was

$0.5cm^2$. Then FTO, ZnO coated glass plate was dried on a hot plate at 60°C for 20 minutes. Finally, the samples were sintered at 450°C for 30 minutes. They were cooled to 70°C.

2.4. Preparation of dye sensitizer solutions

The natural dye was extracted and purified following the procedure reported in literature [21]. The natural dye Henna (*Lawson interims*) was washed with distilled water and then immersed in absolute ethanol at room temperature in the dark for one day to extract the dye. The solids were filtered out and the filtrates were concentrated at 60°C for the use as sensitizers [22, 23].

2.5. Preparation of electrolyte

An electrolyte solution was prepared as reported in the literature [24]. Electrolyte solution was obtained by mixing 0.8gm of KI, 10 ml of acetonitrile and included by 0.127gm of I_2. The solution was stirred for 30 minutes and then stored in a sealed bottle.

2.6. Preparation of counter electrode

To prepare the counter electrode, FTO plates were painted with carbon on the conducting side using a graphite pencil to apply a light carbon film to the entire conductive side of the plate.

2.6.1. Assembly of DSSC

Solar cell was assembled by making paste of 3.5gm of ZnO powder, added by 1ml of acetic acid, 4ml of ethanol, 5ml of distilled water, and two drops of TritonX-100 and then grained by mortar. The paste was then coated on FTO glass which has been made the mode of 0.5×0.5 cm^2 using doctor blade method. After the paste was dried, it was then heated at 450°C for 30 minutes and then it immersed in dye solution for 24 hrs. Another FTO glass plate was coated by using carbon from graphite pencil on its conductive surface. Then two drops of KI/I_2 electrolyte solution wad added into the cell, and then the solar cell performance was measured.

2.6.2. Characterization methods

The structural, optical and photo electrochemical properties have been investigated for prepared photo electrochemical cells. The XRD analysis is measured using Diffract meter system XPERT-PRO. Surface morphology of the prepared films were studied using scanning electron microscope (FE-SEM) (EVO 18 SEM) and the elemental composition of samples were analyzed using energy dispersive x-ray spectroscopy EDAX (QUANTA-FEG 250). The absorption spectra of natural dyes and ZnO thin film were measured using a UV-VIS spectrophotometer (HITACHI UH 5300) in the wavelength range of 200-1100 nm. The absorption measurements of natural dye and ZnO thin film were taken with respect to reference of distilled water and FTO substrate, respectively. FTIR analysis was done using NICOLET IS5 -KBR windows with AR diamond crystal plate. Simulated solar irradiation was provided by a solar simulator, Model PECL01 semiconductor characterization system under the irradiation of AM 1.5 (150 mWcm-2), and the current -voltage curves were analyzed using Keithley electrometer by a digital Keithley multimeter model 6517B/E.

3. RESULTS AND DISCUSSION

3.1. X-ray Diffraction Analysis

The ZnO nanoparticles prepared using the solvothermal method with variation of pH values (3, 6, and 9) are shown in fig. 2.

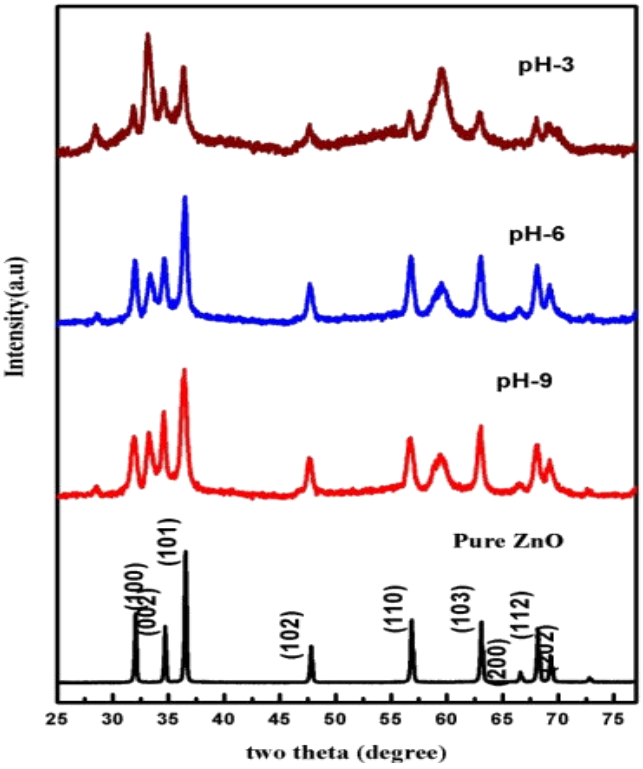

Fig. 1: XRD of ZnO synthesized via the solvothermal method at different pH values i.e. 3, 6 and 9

The sharp and most intense peaks observed here demonstrate that the synthesized ZnO nanoparticles are of high crystalline nature with single phase. The strong

diffraction peaks appear at 33.07 (pH 3), 36.45 (pH 6) and 36.51 (pH 9) corresponding to (101) planes matches well with all peaks show the formation of the hexagonal wurtzite structure of ZnO nanoparticles. The value of pH increases with an increase of 2θ values. This data is with accordance to the JCPDS file no 36-1451.The cell parameters a=b= 3.249, c=5.206 are moreover affirmed by the JCPDS data.

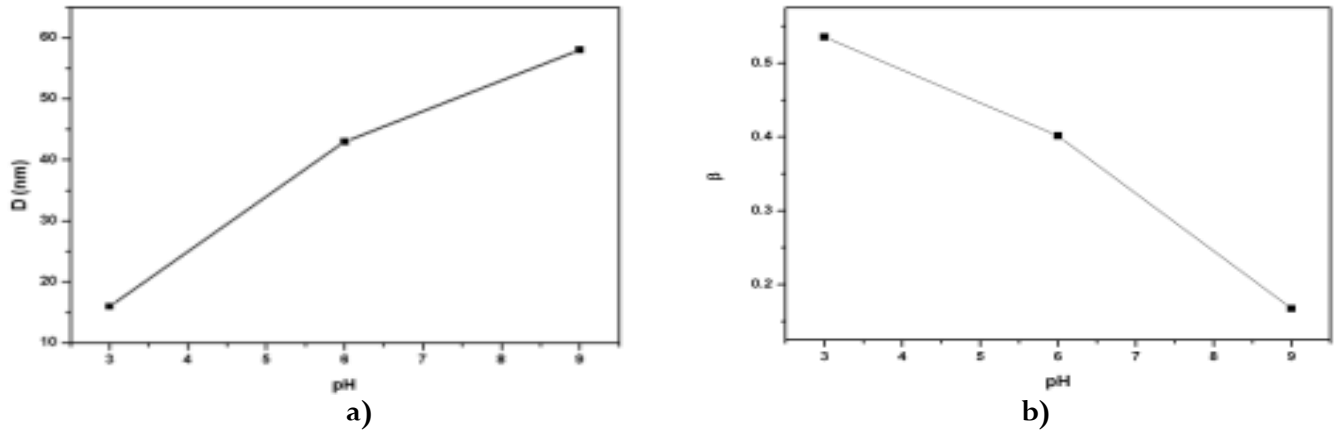

a) b)

Fig. 2: a) The variation of pH versus D and b) pH versus beta

Average crystallite size D for ZnO nanoparticles was calculated using the Debye-scherrer formula which is given in Eqn (1)

$$D = K\lambda/\beta Cos\theta \quad \ldots\ldots\ldots (1)$$

K=0.89 is the Debye Scherrer constant, β is the full width at half maximum, λ is the X-ray wavelength, and θ is the Bragg diffraction angle obtained from 2θ value corresponding to maximum intensity peak in XRD pattern.

The average crystallite size calculated across 29.17nm, 38 nm and 48.63 nm for the samples obtained at ZnO pH 3 and 6 and 9 respectively. The reason that the average crystallite size increases with an increase in the pH value of the solution just like the case of an increase in diameter of the ZnO nanoparticle [25, 26] and also the intensity of planes (102), (110),(103) and (112) increases from pH 3 to 9. Also, it clearly shows that an increase in pH value helps in the nucleation and growth of nanoparticles. The low pH value of 3 and 6 correspond to the acidic nature of the solution and it could restrain the particle growth. When the pH value is above 7, the total alkali environment supports hydrolysis and this enhances particle growth, thereby increasing the particle size [27].

Fig. 2b shows the variation in FWHM of the dominating two theta peak (101) with increasing pH. It can be clearly seen that FWHM decreases on increasing pH which implies the increases in crystalline nature.

3.2. FITR analysis

Fig. 3 shows the FTIR spectrum of ZnO nanoparticle at different pH values. The ZnO peak that appears in the range of 420-390 cm^{-1} shows that the transformation of Zn $(OH)_2$ to ZnO was completed. Past analysis found the ZnO peak between 550-453cm^{-1} [28]. In this study, ZnO peaks of all the samples were moved conflictingly since of the impact in the event that ZnO particles sizes changing with pH. Thus, the particle size affects the peaks shifts [29]. These all peaks were ascribed to Zn-O bonds. The FTIR measurements affirmed the XRD results indicating the formation of ZnO material without any other impurities.

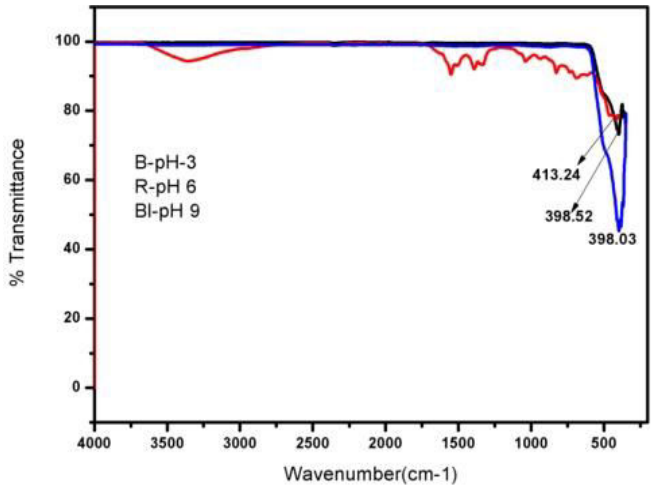

Fig. 3: FTIR spectrum of ZnO nanoparticles synthesized at different pH values

The fig. 4 shows that the chlorophyll dye extracted from henna shows the broad and strong peaks at 3340.37cm^{-1} due to presence of hydroxyl group in stretching vibration mode. C=O stretching vibration shows a peak at 1734.37 cm^{-1}. The peaks at 1368.87 cm^{-1} exhibited the C-N-C bending vibrations. The peaks at 1043.91cm^{-1} and 1043.40cm^{-1} represented the stretching vibrations of C-O-C ester and bending of carbonate is observed at 877.58 cm^{-1}. The functional groups confirmed the presence of chlorophyll [30].

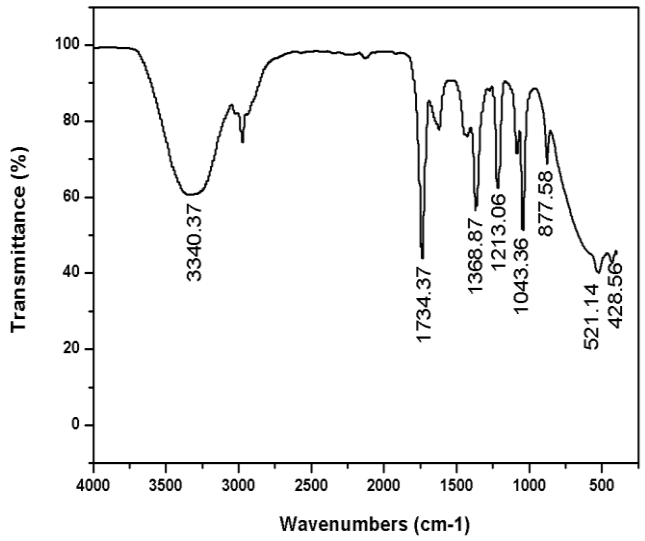

Fig. 4: FTIR spectra of natural dyes extracted from Henna

3.3. Analysis of UV-Visible absorption spectra

The UV-Visible absorption spectrum of natural dye was measured using a UV-Visible spectrophotometer. Fig.5. shows the representative UV-Visible absorption spectra for the extracts of Henna, dissolved in ethanol. It illustrates that the absorption peaks of chlorophyll dye extracted from henna leaves are at 664nm and 286nm. Henna strongly absorbs the photons in UV and visible regions of the wavelength between 250 nm and 700 nm. The band gap energy of the extraction of natural dyes is shown in fig. 6. From the band gap energy using tauc's plot, band gap values is 1.68eV. By decreasing pH value and the extraction temperature of dyes, the efficiency was found to be improved [30]. The lowest band gap energy helps the electron to move fast from the valence band to conduction band and required less energy for the recombination of electron [31]. It shows that the band gap energy of extracted natural dyes is decreasing with the effect of the efficiency of the solar cell.

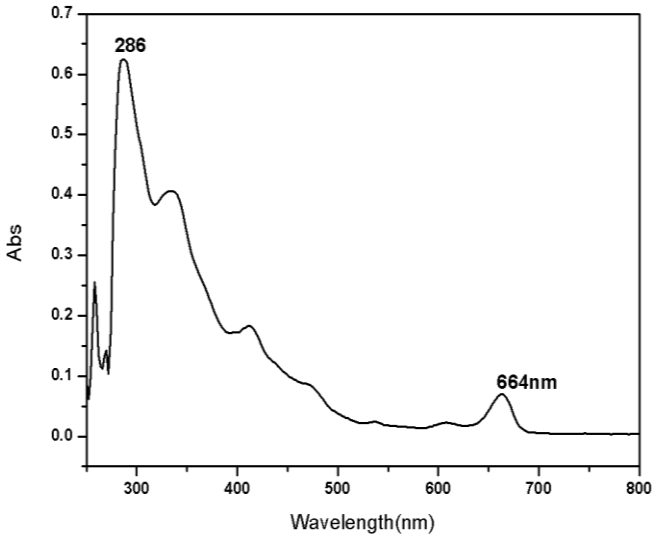

Fig. 5: UV-Visible absorption spectra of dye extracted from Henna

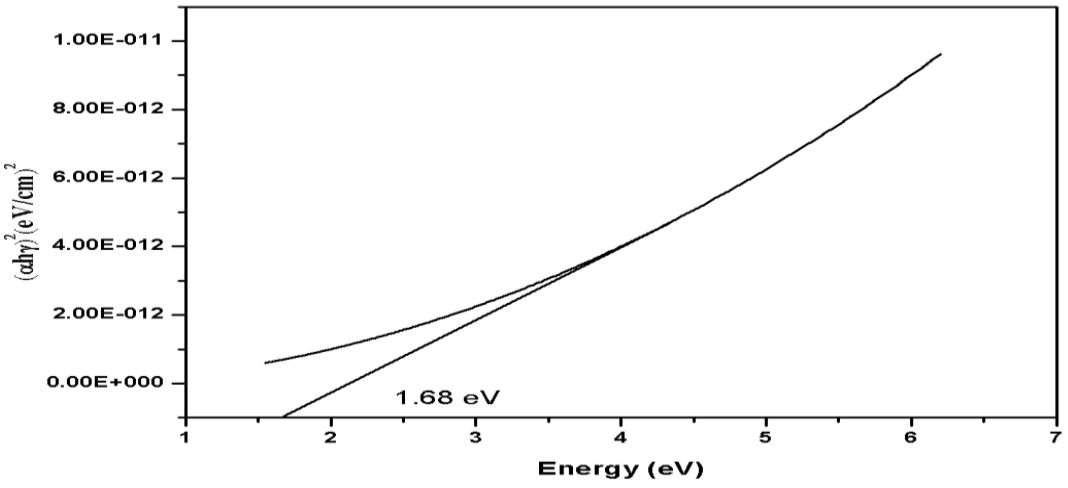

Fig. 6: Tauc's plot of dye extraction from Henna

Fig.7 shows the result obtained from UV-Visible spectrophotometer analysis for synthesized ZnO nanoparticle at various pH values (3, 6 and 9). The absorbance wavelength ranges of ZnO nanoparticles are 200nm-400nm. As can be seen, the absorbance peak increase when the pH increases from 3, 6 and 9 confirmed higher absorbance and sharpness in contrast to other pH due to the fact that intrinsic band gap of ZnO is associated to electron transitions from the valence band to conduction band [32].

The band gap energy of the ZnO nanoparticles can be calculated using the formula as shown in eqn

$E_g = h\nu = hc/\lambda = 1240/\lambda$ .....(2)

Where, E_g = Band gap energy (eV), h = Planck's constant (6.626×10^{-34}Js), ν = frequency of light, c = speed of light (3×10^{8}m/s), and λ = wavelength of light (nm)

From the fig. 8, it is clear that increase of pH value results in increase of particle size but band gap enegy decreases [33]. The pH value and particle sizes are inversely proportional to the band gap energy.

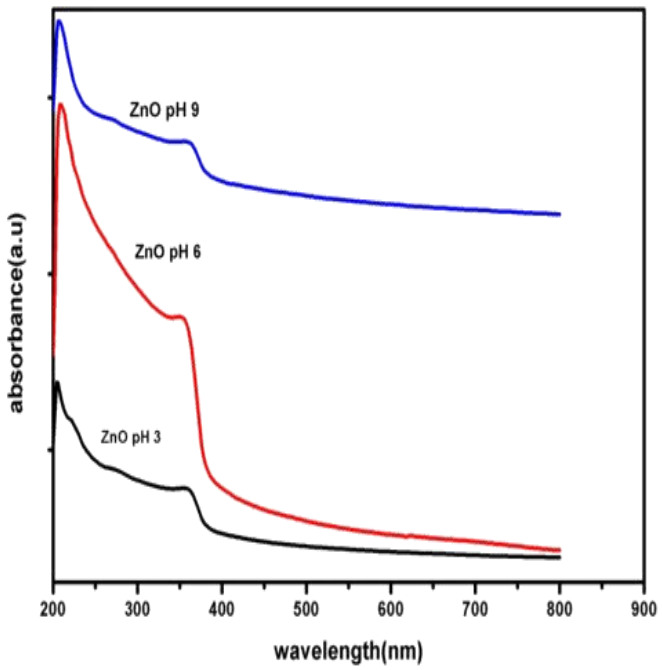

Fig. 7: UV-Visible absorption spectra of ZnO nanoparticles with pH 3, 6 & 9.

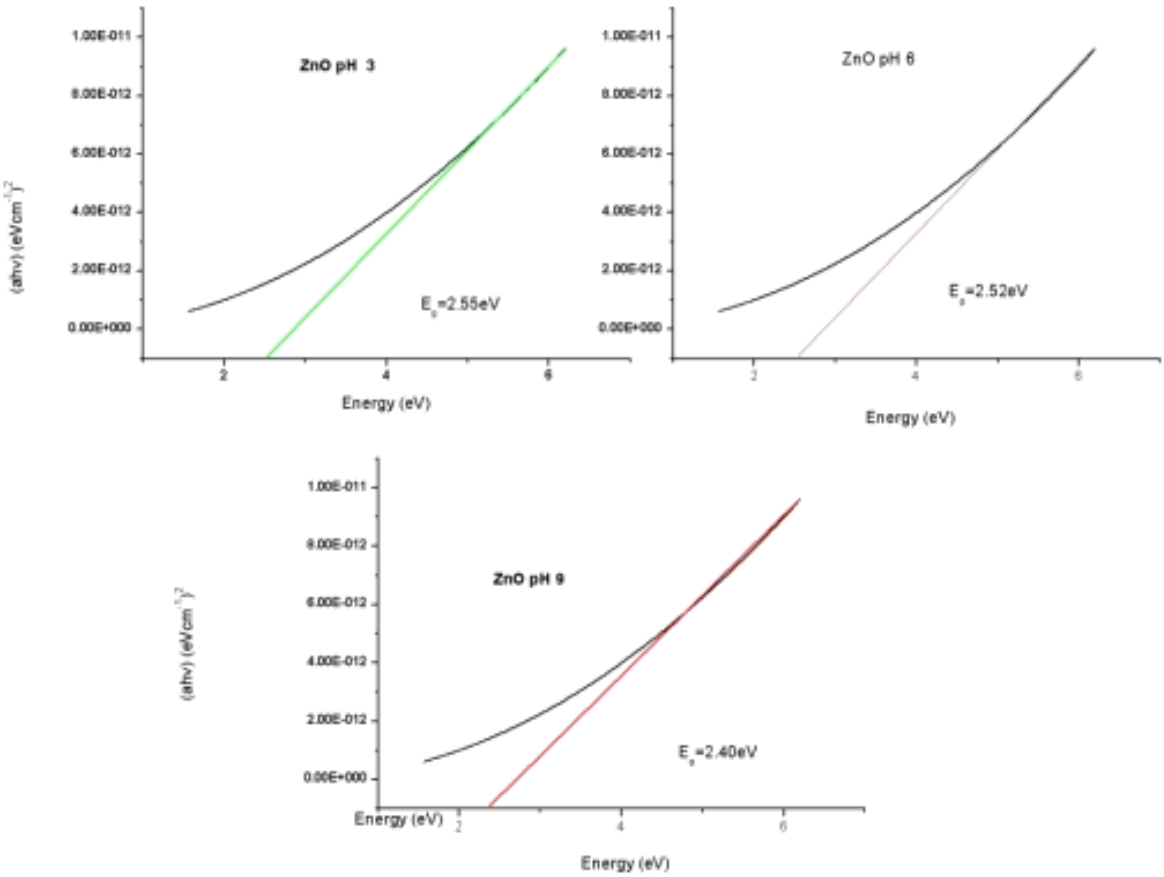

Fig. 8: Bandgap energy (tauc's plot) of the ZnO nanoparticles synthesized at pH 3, pH 6 and pH 9 of ZnO

3.4. Field Emission Scanning Electron Microscopy (FE-SEM) and elemental analysis

Morphology of ZnO nanoparticles synthesized by solvothermal method using microwave irradiation technique is shown in fig. 9. The particle size of synthesized nanoparticels was measured by Image J software. Therefore, the particle size for pH 3 is 22nm, for pH 6 is 31 nm and for pH 9 is 43nm. From the fig., ZnO pH 9 shows that clear hexagonal shape seen in FESEM image consist of a number of crystallites which are seen by the image. The morphology of these particles was hexagons shapes and increase of pH values results in increases of morphology. So pH 9 was very useful for efficiency increase.

The chemical (elemental) composition analysis is very essential to know the exact concentration of elements and defects presents in the photo anodes. The EDX spectrum of ZnO sample shows the presence of Zn and O elements in the sample which confirms the absence of any other impurities [34].

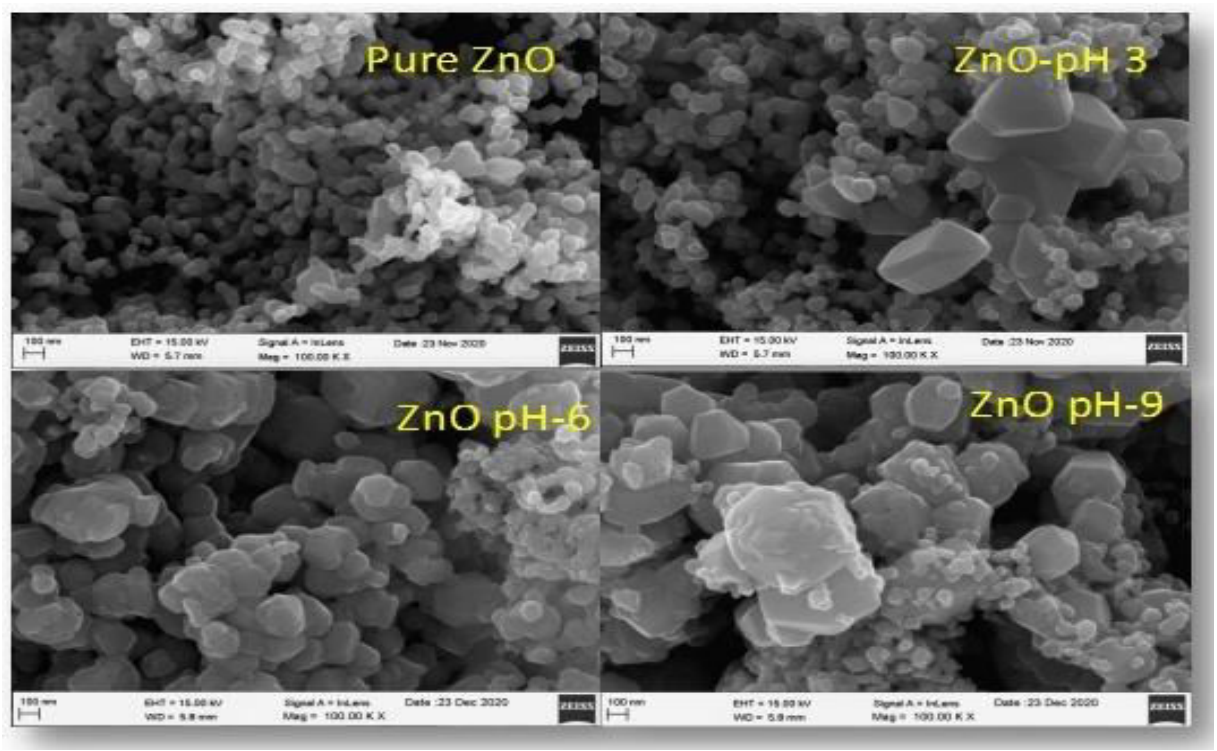

Fig. 9: The FESEM image of ZnO nanoparticles synthesized at pH 3, 6 & 9 using solvothermal technique

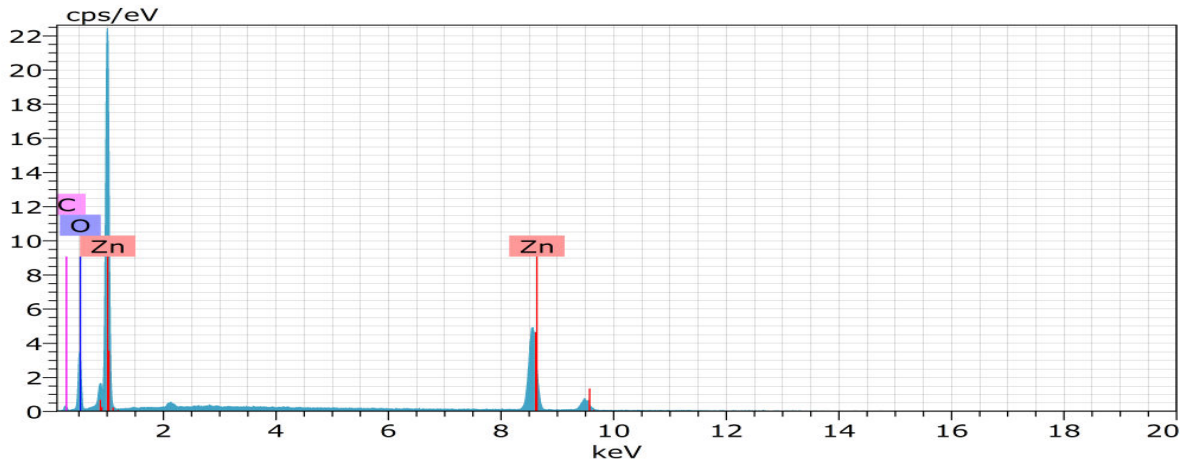

Fig. 10: EDX spectra of ZnO nanoparticle

3.5. IV J-V Characterization of DSSC

The J-V measurement of the fabricated DSSCs was conducted under an illumination of 100mW/cm^2. Fig 11 Illustrates the J-V characteristic curves obtained for the DSSCs sensitized with natural leaves. To evaluate a solar cell performance, short circuit current density (Jsc), open circuit voltage (Voc), Fill Factor (FF) and efficiency (η) should be determined. The fill factor and efficiency are calculated using these parameters. All the photo electrochemical parameters of the fabricated cells are presented in Table 1.

From the table 1, it is seen that Open Circuit voltage (Voc) is 1 V and the short circuit current densities (Jsc) vary from 0.85 to 1.09 mA/cm^2. The highest V_{oc} is 1V and Jsc=1.09 mA/cm^2 were obtained with the DSSC sensitized by the *Lawsonia inermis* leaves extract, the efficiency of which reached 0.36% at ZnO -pH 9 due to the high amount of chlorophyll present in the *Lawsonia inermis* leaf, and the efficiency was high. From the above results it is observed that the photoelectric conversion efficiency of the pH 9 with henna leaves extract is higher than the photoelectric conversion efficiency of other pH values [35]. This is because, pH 9 was better than the other solar cells of pH variations due to higher surface area of ZnO at pH 9 has the advantage of having more dyes represent the SEM images.

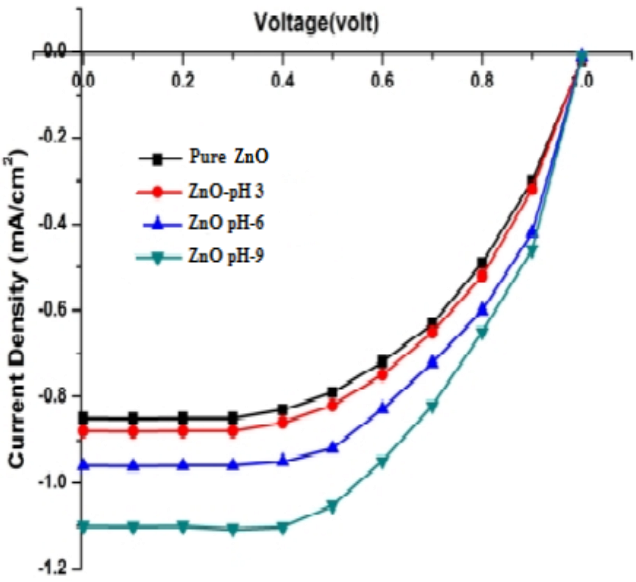

Fig. 11: J-V curves for the DSSCs based on various photo anodes using *Lawsonia inermis*

Table 1: Photoelectrochemical parameters of DSSC using *lawsonia inermis* natural dye

Dyes	V_{oc}(V)	J_{sc}(mA/cm^2)	V_{mp}(V)	J_{mp}(mA/cm^2)	FF	η(%)
Pure ZnO	1	0.85	0.59	0.72	0.49	0.27
ZnO- pH 3	1	0.88	0.56	0.78	0.496	0.29
ZnO- pH 6	1	0.95	0.58	0.85	0.51	0.32
ZnO- pH 9	1	1.09	0.55	0.99	0.499	0.36

Table 2: Photovoltaic performance of DSSC sensitized with different natural dyes

Natural dyes	semiconductor	J_{sc} (mA/cm$^{2)}$	V_{oc} (V)	FF	η (%)	References
Henna	ZnO	3.8	0.33	85	1.08,	36
		0.368	0.426	24.6	0.128	37
	TiO_2	0.84	324(mV)	0.24	0.65	38
		0.407	0.306	28.1	0.117	37
	ZnO	0.98	1	0.47	0.30	

4. CONCLUSIONS

In this report, Dye-Sensitized Solar Cell has been successfully prepared from ZnO material with different pH values of 3, 6 and 9 with Henna were prepared by solvothermal microwave irradiation technique. XRD results show the formation of the hexagonal wurtzite structure of ZnO nanoparticles of different pH values (3, 6 and 9) with uniform distribution. The particle size of the sample increases with pH and band gap energy decreases was concluded using the UV-Visible spectroscopic studies. The lowest band gap energy of the extracted natural dyes is given the better efficiency for DSSC using Tauc's plot. The J-V characteristic curves of the fabricated cells were carried out. The pH 9 henna leaves gives the highest efficiency of 0.39% among other pH variations of photoanodes due to low band gap energy and chlorophyll occurred with photo electrochemical parameters of V_{oc}= 1 V, J_{sc}= 0.98

mA/cm^2, FF= 0.47 and η=0.39%. ZnO nanoparticles synthesized at pH 9 showed 0.39% efficiency and are comparatively better than the ZnO prepared at pH 3 & 6. In the future, efforts will be taken to improve the performance of the DSSC by varying the natural dyes, methods and various parameters mentioned earlier.

5. ACKNOWLEGEMENT

Author E. Selva Esakki would like to express her gratitude to DST FIST Sponsored Centralized Research Facility, Sri Paramakalyani College, Alwarkurichi for providing technical supports.

Declaration of Competing Interest

The authors declare that they have no known competing financial interests or personal relationships that could have appeared to influence the work reported in this paper.

6. REFERENCES

1. O'regan B, Grätzel M. *Nature*, 1991; **353(6346):**737-740.
2. Kumar SS, Venkateswarlu P, Rao VR, Rao GN. *International Nano Letters*, 2013; **3(1):**30.
3. Chen Y, Ding H, Sun S. *Nanomaterials*, 2017; **7(8):**217.
4. Prema latha K, Prema C. *J.Nanosci.Tech*, 2018: **4 (5)**:475-477.
5. Rao KJ, Vaidhyanathan B, Ganguli M, Ramakrishnan PA. *Chemistry of Materials*, 1999; **11(4)**:882-895.
6. Shanmugam V, Manoharan S, Anandan S, Murugan R. *Spectrochimica Acta Part A: Molecular and Biomolecular Spectroscopy*, 2013; **104**:35-40.
7. Garcia CG, Polo AS, Iha NY. *Journal of Photochemistry and Photobiology A: Chemistry*, 2007; **160(1-2):**87-91.
8. Tennakone K, Kumara GR, Kumarasinghe AR, Sirimanne PM, Wijayantha KG. *Journal of Photochemistry and Photobiology A: Chemistry*, 1996; **94(2-3):**217-220.
9. Gallo M, Ferracane R, Graziani G, Ritieni A, Fogliano V. *Molecules*, 2010; **15(9)**:6365-6374.
10. Cortez R, Luna-Vital DA, Margulis D, Gonzalez de Mejia E. *Comprehensive Reviews in Food Science and Food Safety*, 2017; **16(1)**:180-198.
11. Hao S, Wu J, Huang Y, Lin. *J. Solar energy*, 2006 ; **80(2)**:209-214.
12. Guruvammal D, Selvaraj S, Sundar SM. *Journal of Magnetism and Magnetic Materials*, 2018; **452**:335-342.
13. Varadhaseshan R, Sundar SM. *Applied surface science*, 2012; **258(18):**7161-7165.
14. Esakki ES, Sarathi R, Sundar SM, Devi LR. *Materials Today: Proceedings*, 2021; **47**: 2182-2187.
15. Sundar M, Prema C. *Physics Procedia*, 2014; **54**:55-61.
16. John Kennady Vethanathan S, Perumal S, Meenakshi Sundar S, Priscilla Koilpillai D, Karpagavalli S, Suganthi A. *Int. J. Adv. Sci. Tech. Res.*, 2014; **6(3):**856-865.
17. Godibo DJ, Anshebo ST, Anshebo TY. *Journal of the Brazilian Chemical Society*, 2015; **26(1)**:92-101.
18. Xiang Y, Yu J, Zhuang J, Ma Z, Li H. *Solar Energy Materials and Solar Cells*, 2017; **165**:45-51.
19. Zhou H, Wu L, Gao Y, Ma T. *Journal of Photochemistry and Photobiology A: Chemistry*, 2011; **219 (2-3)**:188-194.
20. Cao J, Zhu Y, Yang X, Chen Y, Li Y, Xiao H, Hou W, Liu J. *Solar Energy Materials and Solar Cells*, 2016; **157**:814-819.
21. Taya SA, El-Agez TM, El-Ghamri HS, Abdel-Latif MS. *International Journal of Materials Science and Applications*, 2013:37-42.
22. El-Agez TM, El Tayyan AA, Al-Kahlout A, Taya SA, Abdel-Latif MS. *International Journal of Materials and Chemistry*, 2012 ; **2(3)**:105-110.
23. Agus SG, Irmansyah I, Akhiruddin M. *Журнал нано-та електронної фізики*, 2016; **8(2)**:02012-1.
24. Susanti D, Prasatya AN, Purwaningsih H, Fajarin R, Rohmanuddin TN. *Proceedings of the 3rd Applied Science for Technology Application (ASTECHNOVA 2014),* 2014.
25. Chithra MJ, Sathya M, Pushpanathan K. *Acta Metallurgica Sinica (English Letters),* 2015; **28(3)**:394-404.
26. Alias SS, Ismail AB, Mohamad AA. *Journal of Alloys and Compounds*, 2010; **499(2)**:231-237.
27. sivakumar k, Senthil Kumar V, Muthukumarasamy N, Thambidurai M, Senthil TS. *Bull. Mater.Sci*, 2012; **35**:327.
28. Wahab R, Ansari SG, Kim YS, Dar MA, Shin HS. *Journal of Alloys and Compounds*, 2008; **461(1-2)**:66-71.

29. Ammar AM, Mohamed HS, Yousef MM, Abdel-Hafez GM, Hassanien AS, Khalil AS. *Journal of Nanomaterials*, 2019; 2019.
30. Ganta D, Jara J, Villanueva R. *Chemical physics letters,* 2017; **679:**97-101.
31. Wongcharee K, Meeyoo V, Chavadej S. *Solar Energy Materials and Solar Cells*, 2007; **91(7)**:566-571.
32. Shiyani T, Agrawal S, Banerjee I. *Nanomaterials and Energy*, 2020; 1-2.
33. Wahab R, Ansari SG, Kim YS, Song M, Shin HS. *Applied Surface Science*, 2009; **255(9)**:4891-4896.
34. Mahamuni PP, Patil PM, Dhanavade MJ, Badiger MV, Shadija PG, Lokhande AC, Bohara RA. *Biochemistry and biophysics reports*, 2019; **17**:71-80.
35. Chang H, Wu HM, Chen TL, Huang KD, Jwo CS, Lo YJ. *Journal of Alloys and Compounds*, 2010; **495(2)**:606-610.
36. Sakthivel, Baskaran V, *Int. J. Sci. Res.*, 2014; 93–96.
37. Jasim KE, Cassidy S, Henari FZ, Dakhel AA. *J. Energy Power Eng*, 2017; **11**:409-416.
38. Sakthivel S, Baskaran V. *International Journal of Science and Research,* 2014.